Shinde and Lala
Future Journal of Pharmaceutical Sciences (2023) 9:81
https://doi.org/10.1186/s43094-023-00531-y

Future Journal of Pharmaceutical Sciences

RESEARCH

Open Access

Mannose-anchored solid lipid nanoparticles loaded with atorvastatin calcium and vinpocetine as targeted therapy for breast cancer

Amol S. Shinde[1] and Rita R. Lala[1*]

Abstract

Background This study was aimed to design mannose-conjugated solid lipid nanoparticles (MSLNs) for the targeted delivery of Atorvastatin Calcium (ATS) and Vinpocetine (VIN) to augment its therapeutic efficacy against breast cancer. SLNs were prepared by hot emulsification ultra-probe sonication method and conjugated with mannose. In vitro cell line, in vivo pharmacokinetic and in vivo tumor regression studies were performed for MSLNs.

Results MSLNs had an average particle size of 435.4 ± 3 nm with polydispersity index 0.298 ± 0.03 and a zeta potential of − 28.2 ± 1 emv. Entrapment efficiency was found to be 69.17 ± 0.92%, 71.18 ± 0.68% for ATS and VIN, respectively. The IC50 value of MSLNs was 1.46 µg/ml, which is efficient to control the growth of MDA MB231 cells as compared to the individual drugs and combinatorial SLNs. The combination index was found to be 0.7. MSLNs inhibited cell growth via necrosis by promoting to apoptosis through arresting SubG1 phase. The relative bioavailability of ATS and VIN loaded in MSLNs was 1.47 and 5.70, respectively, as compared to the marketed formulation. Maximal tumor volume reduction and higher survival rate was found for the MSLNs group (76.03%, $P = 0.0001$) as compared to the control group ($P = 0.0364$), individual drugs SLNs group.

Conclusion The results revealed that the MSLNs formulation augmented activity against breast cancer by inhibiting the cell growth. This promising drug delivery reduces the doses for both the drugs and attains minimal dose-associated side effects with synergism by reaching the specific target site, furthermore improving the therapeutic efficacy.

Keywords MSLNs, Conjugated, Cell line, Cell cycle analysis, In vivo tumor regression

Background

Female breast cancer is leading type worldwide in terms of number of new cases; approximately 2.26 million diagnoses are assessed in 2020, contributing about 22.37% of the total cancer incidence burden. Female breast cancer ranks as the 5th leading cause of death (6,85,000 deaths, 6.78%) because the prognosis is relatively favorable, at least in more developed countries [1].

Combinational chemotherapy is preferred for cancer treatment which shows synergistic therapeutic effects and reduce dose associated systemic toxicity by simultaneously it also modulates multiple cell-signaling pathways and overcome the issues of multidrug resistance [2].

Solid lipid nanoparticles (SLNs) are having smaller particle size leading to larger surface area and ability to change their surface area properties, enhance the permeability and retention (EPR) effect. SLNs systems is extensively used as carriers for anticancer agents due to

*Correspondence:
Rita R. Lala
rr.lala@kmkcp.edu.in
[1] Department of Pharmaceutics, Principal K. M. Kundnani College of Pharmacy, Mumbai 400005, Maharashtra, India

its better biocompatibility of lipids than other materials and also it improves drug activity by reaching to the target site, reduce the side effects of drugs by minimal exposure of drug on normal cells [3, 4].

Cancerous cells express the number of receptor cells on the surface that receptor cells having high affinity for carbohydrate molecules and these receptors are familiar as a membrane lectins. Due to this reason, different carbohydrates might be used as a ligand for targeting of chemotherapeutic agents. Lectin receptor-mediated targeting system use interaction of endogenous ligands with different types of sugar moieties like mannose, galactose. Glycotargeting leads to the interaction of specific lectin receptors with carbohydrate ligands. Mannose–cytostatics complexes have been explored, and in several cases, these conjugates showed a selective entry, better activity and reduced toxicity [5].

Lectin receptors are highly expressed on endothelial kupffer cells, alveolar, splenic and peritoneal macrophages, macrophages of brain, show a rapid internalization of mannose tagged drug delivery via mannose receptor mediated endocytosis. Thus, the development of polysaccharide-based conjugation, i.e., mannose with SLNs as a drug delivery carrier might arise as an imminent approach for selective delivery of anti-cancer agents to the tumor tissues [5, 6].

Statins are 3-hydroxy-methylglutaryl (HMG) CoA reductase inhibitor and are used in hyper cholesterolmia. They show additional anticancer activity against a number of cancers alone or in combination with chemo therapeutic drug; thus being used for chemo preventive treatment of cancer [7]. Some mechanisms of statins are inhibition of proliferation, induction of apoptosis, anti-invasion effect and inhibition of autophagy may influence the cell viability and cell cycle through different pathways [8, 9].

ATS belongs to the Biopharmaceutical Classification System (BCS) class II, having low aqueous solubility leading to low oral bioavailability (12%). It also undergoes extensive first pass metabolism. These problems related to solubility can be improved by developing nano-sized formulations and maintaining it in the amorphous state [10]. ATS induces autophagy in T24 human bladder cancer cells [11], and induces PC3 autophagy in prostate cancer by activating LC3 transcription [12].

VIN a semisynthetic derivative of vincamine is extracted from the periwinkle plant. VIN belongs to BCS class II with low oral bioavailability (7%) as a result of slower dissolution rate in the intestinal tract and a significant first-pass effect. It is prescribed for the treatment of cerebral vascular and cerebral degenerative diseases such as Alzheimer's disease [13, 14]. VIN induces cell apoptosis and impairs the migration of strongly metastatic cells [15].

The present research study was aimed at formulating and developing a suitable MSLNs delivery system loaded with ATS and VIN for the treatment of breast cancer with improved therapeutic efficacy. In vitro cell line, flow cytometry analysis and apoptosis studies on human breast cancer cell line MDA MB231, as well as, pharmacokinetic and in vivo tumor regression studies were performed on the rat as model for the conjugated MSLNs.

The proposed conjugated formulation was found to improve the selectivity of drug delivery by targeting tumor cells without affecting the normal cells. It is expected to enhance the therapeutic efficacy by improving bioavailability, also showing sustained effect which may help to reduce the frequency of dose administration. It reduces the burden of side effects like alopecia and the cost of therapy because the proposed combinatorial therapy is affordable. It is an alternative therapy opening a new way for the treatment of breast cancer.

Methods

Materials

ATS and VIN were gifted by SRS Pharmaceuticals Pvt. Ltd. Mumbai and India Glycols, Himachal Pradesh, India, respectively. Precirol ATO5 and Labrasol were provided by Gattefosse Pvt Ltd, Germany. Glycerol Monostearte (GMS) was gifted by Mohini Organics, Mumbai, and Poloxamer188 by Signet Chemical Corporation Pvt Ltd. Mumbai. Tween 80 was obtained from Loba Chemie, Mumbai. Acetonitrile, Methanol HPLC grade were procured from Merck, Mumbai. Other Chemicals and reagents were of AR grade from local suppliers.

Preparation of ATS and VIN loaded SLNs

SLNs were prepared by the hot emulsification ultra-probe sonication method according to Lala et al. [16]. ATS and VIN (4:1 ratio) were weighed precisely and transferred to a beaker containing weighed quantity of GMS (2.25% w/w), Precirol ATO 5 (2.25% w/w) and Tween 80 (1.67% w/v). This blend was melted at 5 °C above the melting point range of the respective solid lipids. Poloxamer 188 (1% w/w) and Labrasol (3.33% w/v) were dissolved in the aqueous phase and heated to 5 °C above its melting point in another beaker. When a clear lipidic phase was observed, the aqueous phase was added drop by drop into the hot lipidic phase and a primary emulsion was prepared. It was homogenized for 10 min at 7000 rpm. After that, probe sonicator was used for ultrasonification of the emulsion (Probe sonicator, PCI, Mumbai, India) at 40% amplitude with frequency 20 kHz for 25 min. The prepared emulsion was chilled in an ice bath to form SLNs. The prepared SLNs were kept at refrigerated condition.

Preparation of mannose complexed conjugated SLNs (MSLNs)

Mannose conjugation was carried out according to the previous methods with slight modifications [5, 17], D-mannose (X μM) was dissolved in sodium acetate buffer (pH 4.0; 0.1 M) and then added to the unconjugated SLNs. This mixture was kept stirred on a magnetic stirrer continuously (Remi, Mumbai, India) by maintaining at an ambient temperature for 2 days to confirm the completion of the reaction. Mannose complexed nanoparticles were dialyzed (dialysis bag; MWCO 12–14 kDa, Himedia, India) against double distilled water (DDW) for 30 min to eliminate unconjugated mannose along with other impurities; the formulation in the refrigerated condition. The MSLNs formulation was confirmed by FTIR spectroscopy. The unconjugated SLNs were also evaluated by FTIR.

Characterization of the formulations

Fourier transform infrared spectroscopy (FTIR)

The SLNs and MSLNs and D-mannose were characterized and confirmed using an FTIR Spectrophotometer (Alpha T, Bruker). The samples were analyzed and spectrums recorded over the range of 4000–400 cm^{-1}.

Particle size (PS), polydispersity index (PDI) and zeta potential (ZP)

The average PS, PDI and ZP of the prepared SLNs and MSLNs formulations were assessed with Horiba Particle size analyzer and Zeta sizer (Horiba Scientific, Japan). Prior to the analysis of the formulations, SLNs, MSLNs formulations were appropriately diluted to yield a proper scattering intensity using double distilled water. Then, the diluted samples were examined at a fixed scattered angle of 173° and temperature 25 °C. The same procedure was followed for the measurement of zeta potential. The experiment was done in triplicate.

Entrapment efficiency (EE) and drug loading (DL)

EE of SLNs and MSLNs formulation were determined by indirect method of analysis. 2 ml SLNs or MSLNs formulations were taken in 2 ml eppendroff tubes and samples were centrifuged at 10,000 RPM for 45–50 min in a refrigerated centrifuge (Eltek Refrigerated centrifuge, Mumbai). The supernatant layer was collected and appropriate dilutions were done by using methanol. The unentrapped drug amount was evaluated using a UV Vis Spectrophotometer at 246 and 273 nm. EE was calculated by using formula

$$\%EE = \frac{\text{Amount of drug added in formulation} - \text{Amount of unentrapped drug}}{\text{Amount of drug added in the formulation}} \times 100$$

% drug loading was estimated from the entrapped drug and considering the added quantity of solid lipid by the stated formula

$$\%DL = \frac{\text{Amount of entrapped drug in the formulation}}{\text{Amount of solid lipid added} + \text{Amount of ATS and VIN added}} \times 100.$$

Transmission electron microscopy (TEM)

TEM was carried out for SLNs and MSLNs to examine their size, shape and surface morphology using JEM 2100F high-resolution transmission electron microscope (HR-TEM 200 kV). SLNs and MSLNs were dispersed in double distilled water and drop of the dispersion was placed on a 200 mesh carbon coated copper grid. The photomicrographs were captured and morphology was perceived at 50X–1.5 MX and 200 kV voltage.

In vitro release in PBS pH 7.4

The in vitro release pattern of ATS and VIN loaded SLNs, combinational suspension and MSLNs were investigated in PBS pH 7.4. 2 ml of SLNs and MSLNs, equivalent to 8 mg and 2 mg of ATS, VIN, respectively, was poured in a pre-soaked dialysis bag and dipped in 200 ml of PBS pH 7.4 for 24 h beaker, stirred at 100 RPM with the temperature at 37 ± 0.5 °C. Samples were withdrawn after the stated time intervals of 0.5, 1, 2, 3, 4, 5,6,7,8, 12 and 24 h and refilled with same volume of media to maintain sink conditions. Samples were appropriately diluted and the drug content in the samples was analyzed by UV–Vis Spectrophotometer at 246 and 273 nm. The experiments were performed in triplicate.

In vitro cell line study

Sulforhodamine B colorimetric assay (SRB) method was used to estimate the anti-tumor activity of the formulation on human breast cancer cell line MDA MB 231. MDA MB231 cell line was grown in RPMI 1640 medium containing 10% fetal bovine serum and 2 mM L-glutamine. For the current screening experiment, cells were inoculated into 96 well micro-titer plates in 100 μL at

plating densities as mentioned above, reliant on doubling time of cell line. After cell inoculation, micro-titer plates were incubated at 37 °C, 5% CO_2, 95% air and 100% relative humidity for 24 h earlier by adding of investigational drugs in the experiment.

Investigational drugs were first dissolved in water at 100 mg/ml and diluted to 1 mg/ml using DMSO and stored frozen preceding use. At the time of drug addition, an aliquot of frozen concentrate (1 mg/ml) was thawed and diluted to 100 µg/ml, 200 µg/ml, 400 µg/ml and 500 µg/ml with complete medium. Aliquots of 10 µl of these different drug dilutions were added to the appropriate micro-titer wells already containing 90 µl of medium, ensuing in prerequisite final drug concentrations, i.e., 10 µg/ml, 20 µg/ml, 40 µg/ml, 50 µg/ml.

After addition of the composite, 48 h plates were kept for incubation at standard conditions and assay was completed by final addition of cold TCA. Cells were fixed in situ by adding gently 50 µl of cold 30% (w/v) TCA (final concentration, 10% TCA) and incubated for 60 min at 4 °C. The supernatant was discarded; plates washed five times with tap water and dried in air. SRB solution (50 µl) at 0.4% (w/v) in acetic acid (1%) was added to each of the wells and plates were incubated for 20 min at room temperature. After staining, unbound dye was recovered and remaining dye was removed by washing five times with 1% acetic acid. The plates were dried in air. Bound stain was consequently eluted with 10 mM trizma base and absorbance was read on a plate reader at a wavelength of 540 nm with 690 nm as the reference wavelength [18, 19].

Percent growth was estimated on a plate by plate basis for test wells relative to control wells. Percent growth was quantified as the ratio of mean absorbance of test well to the mean absorbance of control wells * 100.

Using six absorbance measurements [time zero (Tz), control growth (C), and test growth in presence of drug at 4 concentration levels (Ti)], percent growth was calculated at each of the drug concentration levels. Percent growth inhibition was determined as:

$$[Ti/C] \times 100\%.$$

Data were illustrated as average ± SD. Graph pad prism V5.0 (Graph Pad Software Inc., San Diego, CA, USA) utilizing nonlinear regression analysis were used for calculation of IC 50 values.

In vitro cytotoxicity and synergistic effects

The synergistic effect of SLNs, MSLNs, free ATS and free VIN on MDA MB231 cells was assessed. MDA MB231 Cells were treated with a combinational dose ratio—4:1 of the concentration of loaded drugs. Combination Index (CI) analysis of free drug combination was based on Chou and Talalay method and determined by CompuSyn Software. For each level of Fa (fraction of affected cells), CI values of SLNs and MSLNs were generated. CI value curves were plotted according to Fa. Fa value (0.2 to 0.8) is specified as validated. CI < 1 signifies synergism and CI > 1 exemplifies antagonism, respectively [20].

Cell cycle analysis (flow cytometry analysis)

Cell cycle distribution based on DNA contents was investigated for human breast cancer cell line MDA MB231 by performing flow cytometry analysis. MDA MB231 cells were plated at a density of 2×10^5 in a 6 welled plate. After 24 h, cells were treated with different formulations and their respective 50% of IC 50 values (free ATS, VIN, ATS SLNs, VIN SLNs, SLNs, and MSLNs) and incubated for 48 h. Then cells were washed with PBS, trypsinized and the cell pellets collected. These pellets were washed with ice cold PBS and centrifuged at 3000 RPM for 3 min. They were fixed with ice cold 70% ethanol. They were incubated in ice for 45 min and again rehydrated with 1 ml PBS and centrifuged. One more PBS wash was given by adding 1 ml PBS, centrifuged and excess PBS was removed. The cell pellet was resuspended in 100 µl of PBS containing RNase A (1 mg/ml) (Sigma, #R6513) for 30 min. 10 µl of propidium iodide (1 mg/ml) (Sigma, #P4170) was added followed by an incubation of 15 min in the dark. Then the volume of entire reaction was made up to 500 µl using PBS and analysis was carried out by flow cytometer (BD FACS Aria system, USA). The cell cycle distribution in the phases of SubG1, G0/G1, S, and G2/M were examined and results were noted. The experimentation was performed in triplicate.

Cell apoptosis analysis by flow cytometry using annexin V-FITC staining

MDA MB231 cells were plated in 6 welled plates at a density of 2×10^5 and incubated overnight. Then they were incubated for 48 h with the respective formulations and their respective 50% of IC 50 values, i.e., free ATS, VIN, ATS SLNs, VIN SLNs, combinatorial SLNs, MSLNs. Cells were trypsinized and washed with prechilled PBS and resuspended with100µl of 1×binding buffer with 5 µl of Annexin V-FITC and 5 µl of Propidium iodide (Abgenex, #1001 K) for 15 min in the dark. Then 400 µl of binding buffer was added and the cells filtered through a cell strainer and analyzed using flow cytometer (BD FACS Aria system, USA) scanner. The experimentation was performed in triplicate.

In vivo pharmacokinetic study

Animal studies were conducted in accordance with procedures approved by Institutional Animal Ethics

Committee (reference number KMKCP/IAEC/192007). To study the plasma concentration time profile for the developed formulations in animals and estimate the bioavailability of the formulation a pharmacokinetic study was performed. Sprague Dawley (150–200 gm) rats were used for the study. Rats were accustomed in the animal house for seven days prior to the experiments under constant environmental conditions (22 ± 3 °C; 50 ± 5% relative humidity) of light/dark cycle of 12 h with free access to standard food and water.

The rats were divided into three groups each containing twelve animals. All the groups were administered with the respective oral marketed formulations (Lipvas and Cognitol tablets), SLNs formulation and MSLNs formulation at a dose of 25 mg/ kg and 6 mg/kg of ATS and VIN, respectively, and 25 mg/kg and 6 mg/kg of both the marketed formulations, respectively. Blood samples were withdrawn from three rats at two time points with gap of 5.5, 7, 10 and 20 h. Blood samples were collected from the retro orbital plexus of the rat eye using fine heparinized capillary and collected in a test tube at fixed time points of 0.5, 1, 2, 4, 6, 8, 12 and 24 h. The collected blood samples were centrifuged at 10,000 rpm for 30 min for separation of plasma. After each withdrawal 1 ml of dextrose normal saline was interposed to partially compensate the electrolyte level and central compartment volume. Collected plasma samples were stored at − 20 °C till analysis.

HPLC method for plasma analysis

1000 µl plasma sample was transferred in to 5 ml test tube. 0.1 ml of buffered solution was added and vortexed for 1 min. 2 ml ethyl acetate was added again vortexed for 2 min and centrifuged at 2500 rpm for 10 min. To the supernatant 1 ml of ethyl acetate was added, transferred in a dry glass test tube and dried at 40 °C, reconstituted with 0.5 ml mobile phase, injected into HPLC system and quantified. Chromatographic analysis was carried out using the stationary phase, reverse phase thermo: BDS Hypersil C18 column. HPLC column of dimensions 250 × 4.6 mm, 5 µm Size. The column oven temperature was kept at 40 °C. A flow rate of 1 ml/min of mobile phase was maintained. The injection volume was 100 µl and the eluate was analyzed by using UV detector with dual wavelength set at 246 and 273 nm. Acetonitrile: Buffer (0.2 M ammonium acetate) [60:40] was used as the mobile phase.

Pharmacokinetic parameters

Maximum concentration C_{max}, time to reach maximum concentration (T_{max}), Area under curve $AUC_{0.5-24}$ (mg.hr/ml), AUC_0-_∞ (mg.hr/ml) were determined by using WinNonlin version 6.3 (Pharsight, Certara, USA) software.

The relative bioavailability of SLNs formulations was calculated using the following equation

$$\%Fr = AUC_t/AUC_r \times 100$$

where Fr: relative bioavailability, AUC_t: area under the plasma concentration–time curve of test, AUC_r: area under the plasma concentration–time curve of reference samples [21].

In vivo tumor regression studies

Animal studies were conducted in accordance with procedures approved by Institutional Animal Ethics Committee (reference number RP 23/2021). In vivo antitumor tumor regression studies were performed to assess the efficacy of the developed formulations on SD rats as the animal model. Human breast cancer was induced by chemical induction method by using 7, 12-Dimethylbenz (a) anthracene (DMBA) and dose was 7.5 mg/kg. IG route was used for administration and the dose was given up to one month when the tumor formed and reached to the required size (20–30 mm^3). Tumor growth was measured using a vernier caliper. Then animals were divided in to seven groups comprising of eight animals each:

Group I—DMBA Control; Group II—Blank SLNs Control; Group III—ATS SLNs (25 mg/kg)
Group IV—VIN SLNs (6 mg/kg); Group V—SLNs [ATS (25 mg/ kg) + VIN (6 mg/kg)]; Group VI—Combinatorial MSLNs [ATS (25 mg/ kg) + VIN (6 mg/kg)]; Group VII—Marketed Tablet Formulation [ATS (25 mg/ kg) + VIN (6 mg/kg)].

All the groups were administered their respective dose of formulations (except vehicle control and blank SLNs control group) ATS SLNs (25 mg/ kg), VIN SLNs (6 mg/ kg), SLNs, MSLNs formulations and marketed formulations at a dose of 25 mg/ kg and 6 mg/kg of ATS and VIN, respectively, daily thereafter, for a total of 28 days. On 29^{th} day, the animals were sacrificed, dissected and the liver, kidney and tumor were carefully collected, measured, processed and observed under a photomicroscope for histopathological examination.

Tumor volume was measured by the following formula

$$\text{Tumor volume}\left(mm^3\right) = \text{length(mm)} \times \left[\text{width(mm)}^2\right] \times 0.5.$$

Stability studies

Combinatorial MSLNs formulation was stored at refrigerated (4 ± 1 °C) and room temperature (25 ± 1 °C) conditions for 3 months. The formulations were analyzed after

specific intermissions 1, 2 and 3 months for PS, PDI, and% EE.

Statistical analysis

All the results were expressed as mean ± SD by performing experiment in triplicate. Statistical analysis was performed with Graph pad prism (version 5.00; Graph Pad Software, San Diego, CA) using two-way ANOVA, one-way ANOVA test or two tailed sample *t* test. $P < 0.05$ reflected that statistically results are significant.

Results

Characterization of combinatorial conjugated MSLNs

Conjugation was accomplished by ring opening of mannose and subsequent reaction of its aldehyde group with free amine functional groups which are present over the surface of unconjugated SLNs in acetate buffer (pH 4). This was due to the formation of Schiff's base (–N CH–). Schiff's base may be get reduced to secondary amine (–NH–CH2) which can be identified by FTIR analysis. Broad intense peak of O–H stretch and C–O stretch of mannose was detected around 333.7 $cm^{-1}$and 1095.61 cm^{-1}, respectively, and N–H deformation of secondary amine at 1470.35 cm^{-1} which confirmed the formation of Schiff's base and amine formation in the linkage between aldehyde from mannose and amine termination groups of SLNs shown in Fig. 1. Similar results were attained in the studies shown by Jain et al. [5] and Sahu et al. [22].

Table 1 Average PS, PDI and ZP of SLNs and MSLNs

Parameters	SLNs	MSLNs
PS (nm)	329 ± 6	435.4 ± 3
PDI	0.321 ± 0.07	0.298 ± 0.03
ZP (− emv)	− 29.8 ± 2.5	− 28.2 ± 1

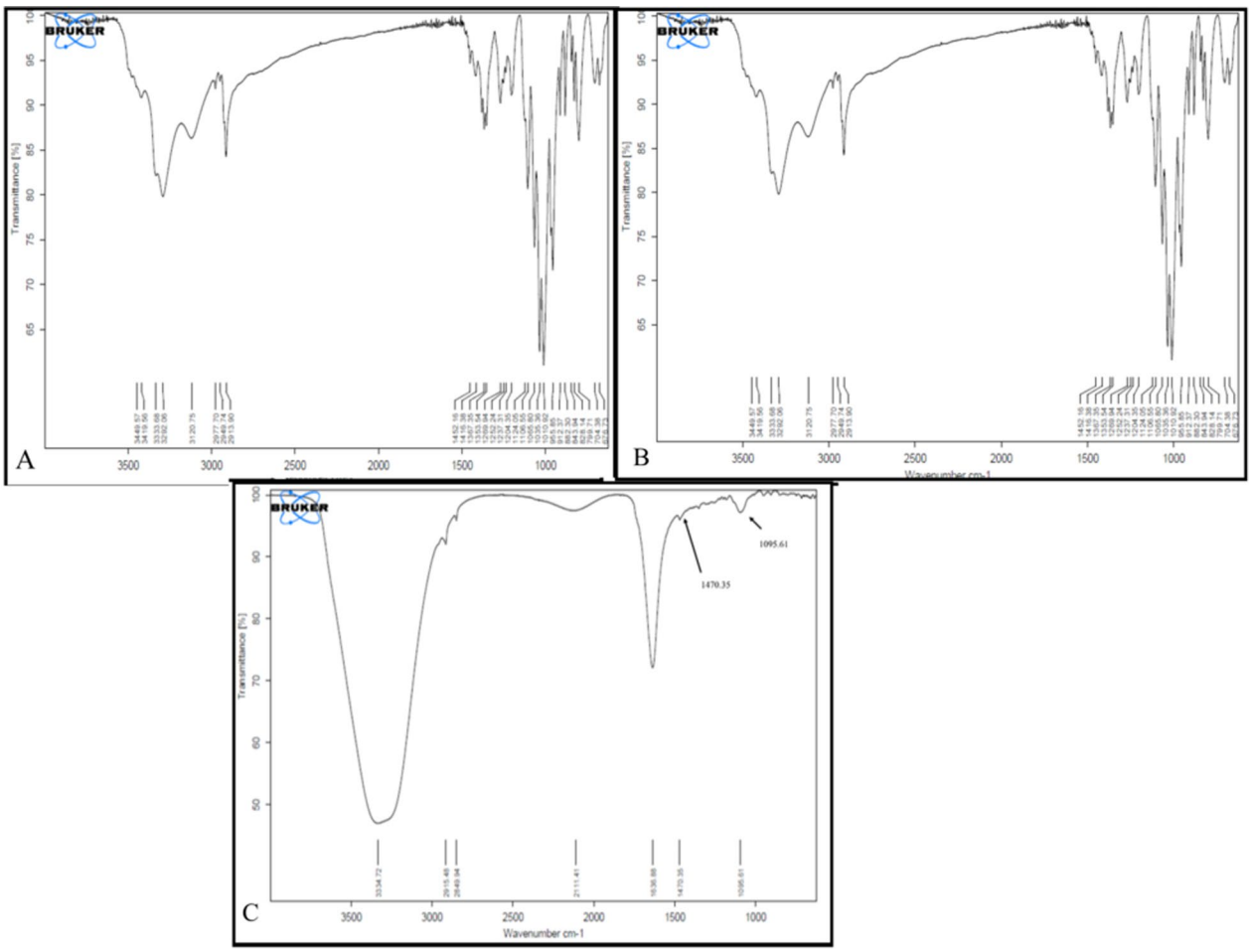

Fig. 1 FTIR spectra, **A** D mannose, **B** SLNs, **C** MSLNs

Particle size, polydispersity index and zeta potential

The particle size of SLNs was 329 ± 6 nm and after conjugation it was 435.4 ± 3 nm. PS, PDI, ZP of SLNs and MSLNs is shown in Table 1. PDI of SLNs and MSLNs was found to be 0.321 and 0.298, respectively. There was slight difference found in the PDI due to stirring which may have decreased the PDI of SLNs when kept for conjugation. ZP of SLNs and MSLNs was − 29.8 ± 2.5 and − 28.2 ± 1 emv.

Entrapment efficiency and drug loading

EE of SLNs was found 65.12% and 67.45% for ATS and VIN, respectively, whereas MSLNs showed 69.17% and 71.18% for ATS and VIN, respectively. DL was found 6.38 and 6.96 for SLNs and MSLNs, respectively. The results of EE and DL of SLNS and MSLNs are shown in Table 2.

Table 2 EE and DL of SLNs and MSLNs

Parameters	SLNs	MSLNs
% EE (ATS)	65.12 ± 1.32	69.17 ± 0.92
% EE (VIN)	67.45 ± 1.58	71.18 ± 0.68
% DL	6.38 ± 1.2	6.96 ± 0.8

Transmission electron microscopy (TEM)

TEM photomicrographs of SLNs and MSLNs are shown in Fig. 2. Both formulations were spherical in shape. Photomicrographs clearly exhibited that the size increased after conjugation with mannose.

In vitro release in PBS pH 7.4

The sustained release behavior of drug molecules was perceived up to 24 h due to diffusion of drug through the lipid core of the SLNs and thus, it influenced the retention time of the drugs in the intestine. Combinatorial suspension showed 47.5% ATS release, SLNs formulation showed 87.38% release up to 24 h whereas MSLNs exhibited 73.75% release. Simultaneously VIN also showed 41.76%, 89.26% and 76.9% release up to 24 h for the combinatorial suspension, SLNs and MSLNs, respectively. The in vitro release studies of both drugs are shown in Fig. 3.

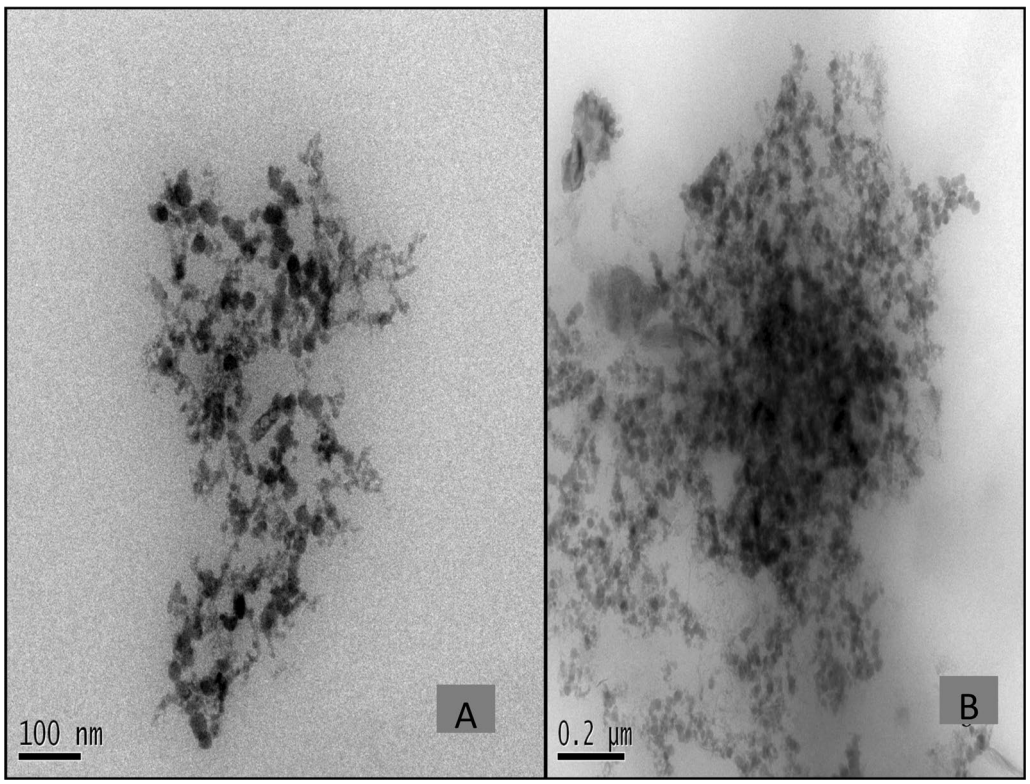

Fig. 2 TEM images, **A** SLNs, **B** MSLNs

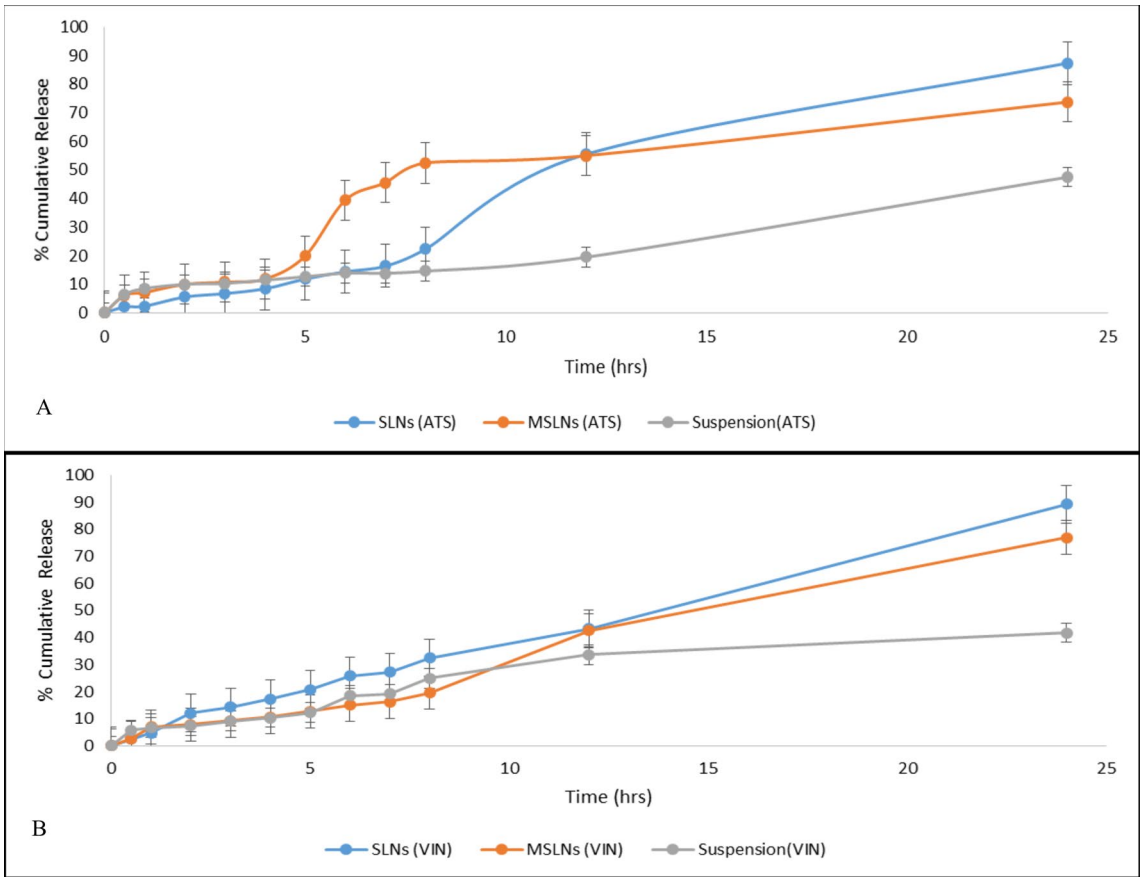

Fig. 3 In vitro release pattern, **A** ATS in PBS pH 7.4, **B** VIN in PBS pH 7.4

Table 3 IC 50 values of MDA MB-231 cancer cell line

Formulations	IC 50 (µg/ml)
Free ATS	25.45
Free VIN	160.9
ATS SLNs	11.66
VIN SLNs	5.81
SLNs	0.88
MSLNs	1.46

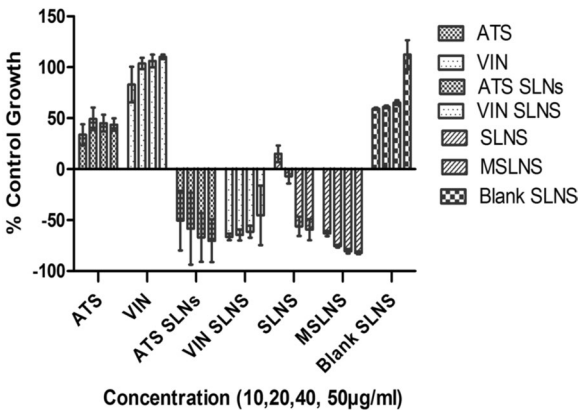

Fig. 4 Growth curve: MDA MB-231 human breast cancer cell line

In vitro cell line study

SRB assay was carried out with free ATS, free VIN, blank SLNs, SLNs and MSLNs at 10, 20, 40 and 50 µg/ml drug concentrations. The MSLNs formulation showed IC 50 values of ATS and VIN for MDA MB231 at very low concentration (1.46 µg/ml), which is highly effective against cancer cell lines compared to free drugs, ATS SLNs, VIN SLNs. There was no significant difference between IC50 values of SLNs and MSLNs. IC 50 values are stated in Table 3. The growth curve of human breast cancer MDA MB231 is shown in Fig. 4.

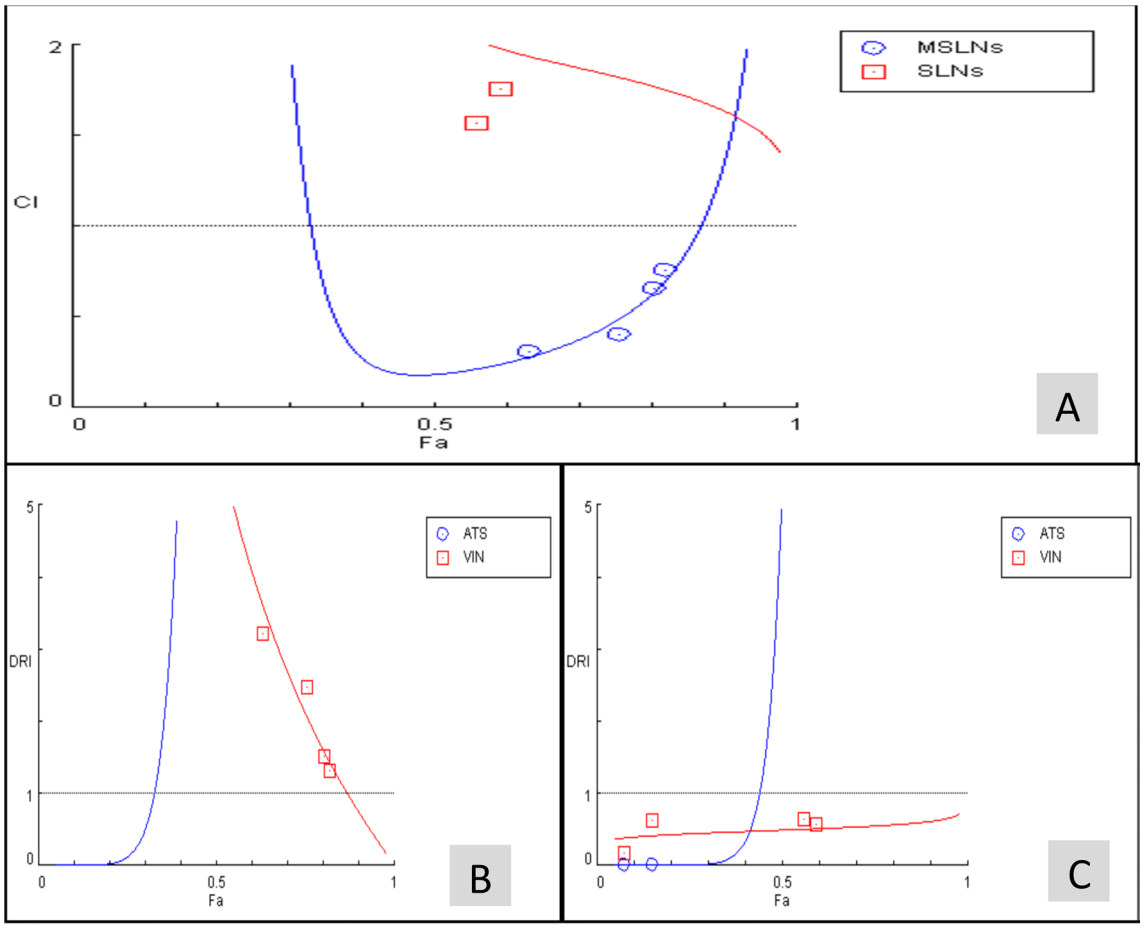

Fig. 5 Synergistic effect of SLNs and MSLNs, **A** Fa-CI values of SLNs and MSLNs, **B** DRI plot of SLNs, **C** DRI plot of MSLNs

In vitro cytotoxicity and synergistic effects

1 > CI value of SLNs and MSLNs is displayed in the Fa–CI plot (Fig. 5). MSLNs exhibited an overall CI value < 1 when Fa value was between 0.2 and 0.8, indicating the appreciable synergy effects of SLNs systems and conjugated MSLNs. CI value was for MSLNs was 0.21 to 0.70, hence MSLNs formulation showed synergistic effect as compared to SLNs. SLNs did show synergistic effect, but it required a higher concentration of dose and CI value was 0.97 (Table 4).

Table 4 CI values of SLNs and MSLNs

Total dose (µg/ml)	SLNs		MSLNs	
	Fa	CI	Fa	CI
10	0.15	1509	0.63	0.21
20	0.25	256.3	0.75	0.33
40	0.56	0.98	0.80	0.58
50	0.67	0.97	0.82	0.70

Cell cycle analysis (flow cytometry assay)

The percent of cells in Sub G1 phase increased compared to Free ATS but there was no significant change in free VIN. In the same manner, ATS SLNs (5.3%) and VIN SLNs (4.4%) individually arrested the cell cycle in Sub G1 phase effectively as compared to the control (4.1%). There was no significant difference found between SLNs (4.8%) and MSLNs (4.7%), but both formulations showed slight cell cycle arrest in Sub G1 phase at very minute concentrations which itself proved the efficacy of combinatorial formulations in arresting the cell cycle synergistically and inhibit cell growth. The concentrations are very low compared to the free drugs and the cells are arrested effectively when individual drugs are encapsulated in SLNs as

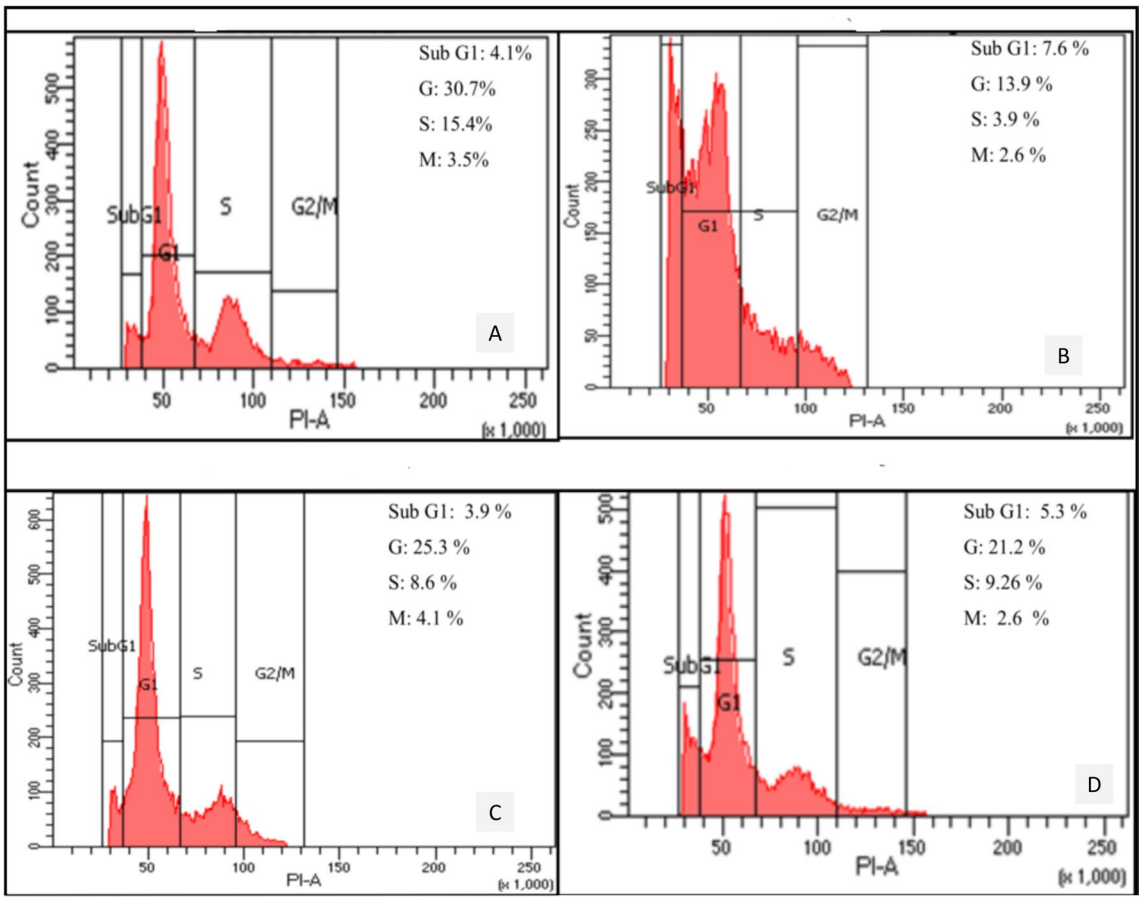

Fig. 6 Effect on MDA MB-231 cell cycle, **A** control, **B** free ATS, **C** free VIN, **D** ATS SLNs

well as in SLNs, or conjugated MSLNs. DNA content is reduced in individual drugs and combinatorial formulations when compared with the control. There was 1.17 fold and 1.15 fold increment in Sub G1 (apoptotic cells) phase. Reduction of cell number was found in S phase for SLNs (10.4%) and MSLNs (7.5%) compared to control (15.4%) at lower concentration, i.e., 50% IC 50. Also, in G2/M phase, number of count for individual drugs, individual SLNs and MSLNs (2.7%) decreased compared to the control (3.5%). Slight increment was observed for SLNs (4.2%) and free VIN. The concentrations used for study and cell cycle distributions are shown in (Figs. 6, 7) with their results.

Cell apoptosis analysis by flow cytometry using annexin V-FITC staining

MDA-MB-231 cells were treated with different formulations and specified concentrations of individual drugs and their combinatorial SLNs, MSLNs for 48 h. These concentrations and results of cell apoptosis are shown in (Figs. 8, 9). Apoptotic cells were determined by flow cytometry using Annexin V- PI staining. Compared to the control only free ATS (12.5 µg/ml) has caused an increase in late apoptosis while other drugs are not displaying any apoptosis. SLNs (0.44 µg /ml), MSLNs (0.73 µg /ml), Free ATS (12.5 µg /ml) and Free VIN (81 µg /ml) exhibited higher necrosis. The concentrations of SLNs, MSNs are very low compared to free ATS, but it still showed 1.55 fold and 1.48 fold necrosis, respectively, compared to the control which is 2.9%. There is no major difference found for apoptosis with SLNs (late apoptosis – 17.5%, early

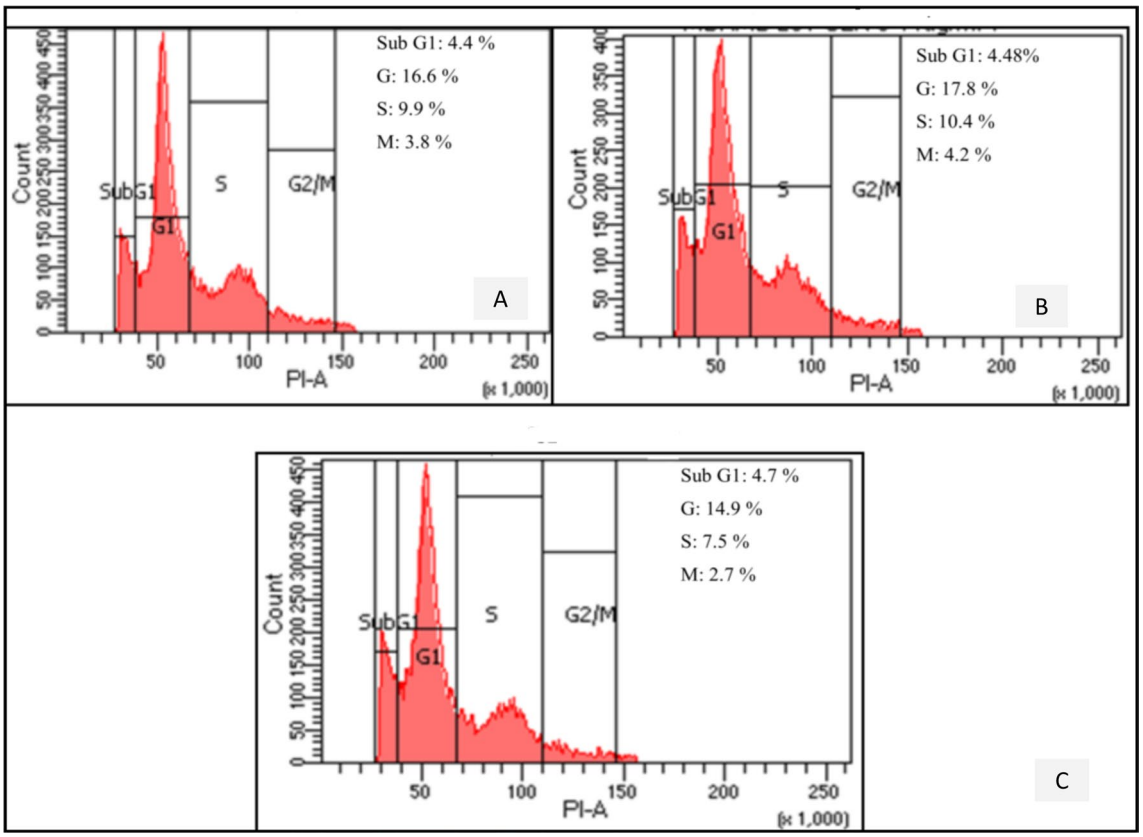

Fig. 7 Effect on MDA MB-231 cell cycle, **A** VIN SLNs, **B** SLNs, **C** MSLNs

apoptosis – 7.6%), MSLNs (late apoptosis – 17.3%, early apoptosis – 7.6%) compared to the control (late apoptosis – 19.8%, early apoptosis – 8.9%). Also, there is no significant difference found for SLNs and MSLNs—both showed the same efficacy against MDA-MB-231 cells.

In vivo pharmacokinetic study

Pharmacokinetic studies were performed on SD rat by administering SLNs, MSLNs and marketed formulations. The unknown concentrations of SLNs, MSLNs and marketed formulations in rat plasma were quantified by a validated HPLC method. The calculated pharmacokinetic parameters are depicted in Table 5 and the mean plasma concentration vs time profiles are shown in Fig. 10.

C_{max} of marketed formulation for ATS and VIN was 10.91 and 0.48 mg/ml whereas T_{max} was found to be 1.93 and 1.87 h for ATS and VIN. C_{max} of SLNs and MSLNs was found to be 22.79, 23.1 mg/ml for ATS and 3.31, 2.28 mg/ml for VIN, respectively. 2.07, 2.05 h T_{max} of SLNs for ATS and VIN whereas 2.21, 2.15 h T_{max} for MSLNs of ATS and VIN. The C_{max} of ATS was increased 2.50 fold in SLNs and 2.12 fold in MSLNs when compared to the marketed tablet formulation. In the same manner C_{max} of VIN was increased 6.90 fold in SLNs and 4.75 fold in conjugated MSLNs. This was possibly due to the nano-size formulation which may have helped to increase the surface area and thus, augment the solubility and dissolution rate [23]. There was no significant difference found between for T_{max} but SLNs and MSLNs showed higher C_{max} in the same period for both drugs which is an advantage of developed formulation.

$AUC_{0.5-24}$ of ATS for SLNs, MSLNs and marketed tablet formulation was 382.513, 336.535 and 140.555 mg hr/mL, respectively. Also, $AUC_{0.5-24}$ of VIN for SLNs, MSLNs and marketed tablet formulation was 12.796, 9.816 and 1.473 mg.hr/mL, respectively. $AUC_{0.5-24}$ showed significant results for MSLNs and SLNs with respect to the marketed tablet formulation. The relative bioavailability was calculated for MSLNs considering the marketed formulation as a reference. The relative bioavailability was 1.47 fold and 5.70 fold increased for

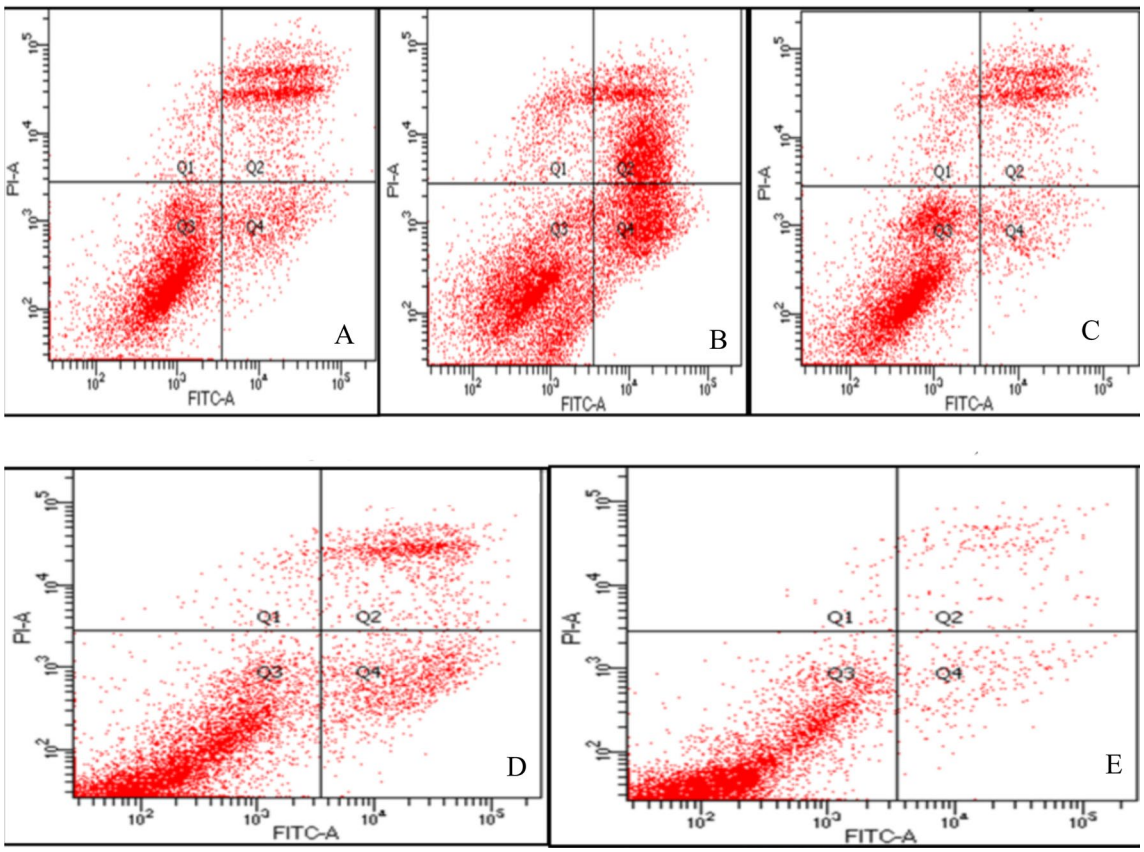

Fig. 8 Apoptosis by annexin V FITC staining on MDA-MB 231, **A** control, **B** free ATS, **C** free VIN, **D** ATS SLNs, **E** VIN SLNs

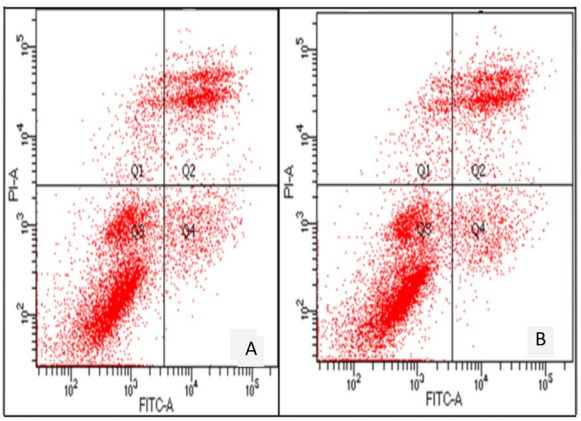

Fig. 9 Apoptosis by annexin V FITC staining on MDA MB-231, **A** SLNs, **B** MSLNs

ATS and VIN in the MSLNs formulation with respect to marketed tablet formulation. These results clearly revealed that the bioavailability and residence time of ATS and VIN increased as compared to marketed tablet formulation.

In vivo tumor regression studies

In vivo anti-tumor regression analysis studies of SLNs and MSLNs were performed. VIN SLNs group ($P=0.0334$) showed lesser tumor reduction during treatment compared to ATS SLNs group ($P=0.0058$). A significant reduction of tumor mass was observed for MSLNs group ($P=0.0001$, 76.03%) as compared to the control group due to the large amount of drug available at the tumor site and with the drug being retained for a prolonged time. Also, the SLNs group showed 63.43% ($P=0.0005$) reduction in tumor mass. The survival rate was 87.5% for all test groups, 75% for control, blank SLNs and marketed formulation group. The liver, kidney and tumor tissue were examined for histopathology. The results of tumor volume results during treatment, inhibition rate (%) and histopathology are shown in Figs. 11, 12, 13, 14 and 15. Mild to moderate changes were observed for SLNs and MSLNs group. Presence of multiple foci of necrotic and degenerative foci in the tumor mass with cellular destruction of neoplastic cells were observed.

Table 5 Pharmacokinetic results of ATS and VIN subsequent single oral dose administration of SLNs, MSLNs and marketed tablet formulation {ATS (25 mg/kg), VIN (6 mg/kg)}

Pharmacokinetic parameters	SLNs		MSLNs		Marketed	
	ATS	VIN	ATS	VIN	ATS	VIN
C max (µg/ml)	27.29	3.31	23.1	2.28	10.91	0.48
T max (hr)	2.07	2.05	2.21	2.15	1.93	1.87
AUC0.5–24 (mg hr/ml)	382.513	12.796	338.535	9.816	140.555	1.473
AUC0-∞ (mg hr/ml)	786.806	13.68	668.986	9.90	451.410	1.734
Relative bioavailability					1.47	5.70

Each value stated as an average ± SD ($n = 3$)

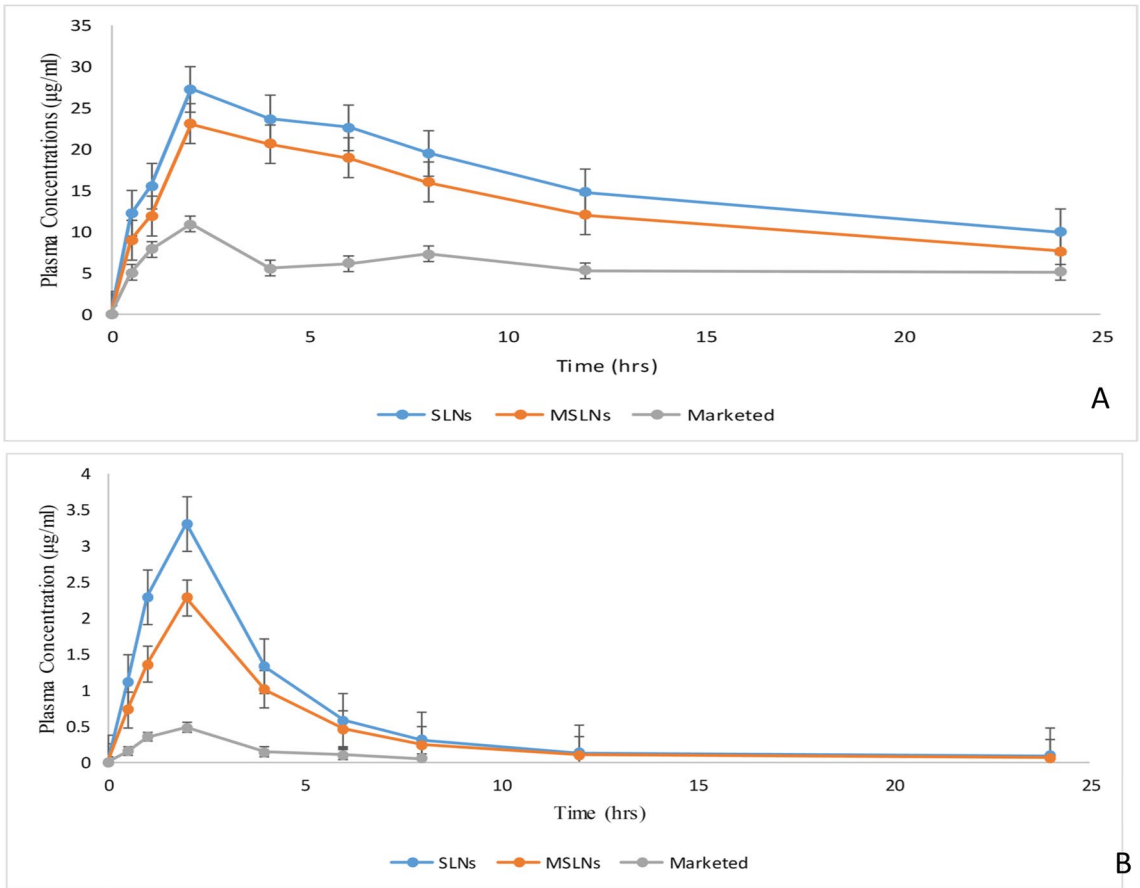

Fig. 10 Mean plasma concentration vs time profile of SLNs, MSLNs and marketed tablet formulation after single oral dose administration of ATS and VIN

Few foci showed marked necrotic changes with destruction of tumor tissue resulting in cellular debris and formation of cystic foci which might be due to treatment given. There was no abnormality found for the liver and kidney in all the groups.

Stability studies

MSLNs was assessed after specific intermissions for stability studies at room temperature and refrigerated conditions. There was an alteration in PS from 435.4 to 513.4 nm, PDI changed from 0.298 to 0.39 under refrigerated conditions after 3 months whereas at room temperature after 3 months PS was 590.5 nm and PDI was

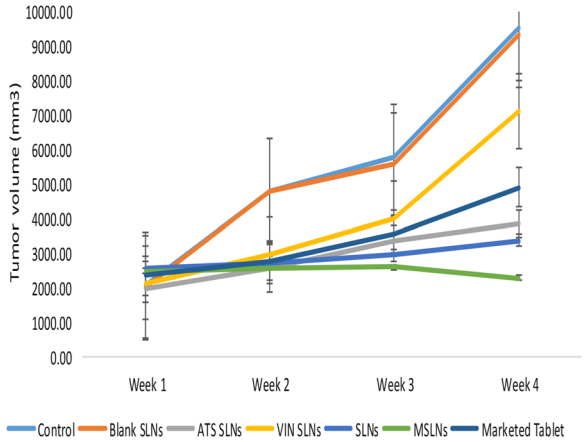

Fig. 11 Therapeutic effect of different formulations on tumor bearing rats during treatment

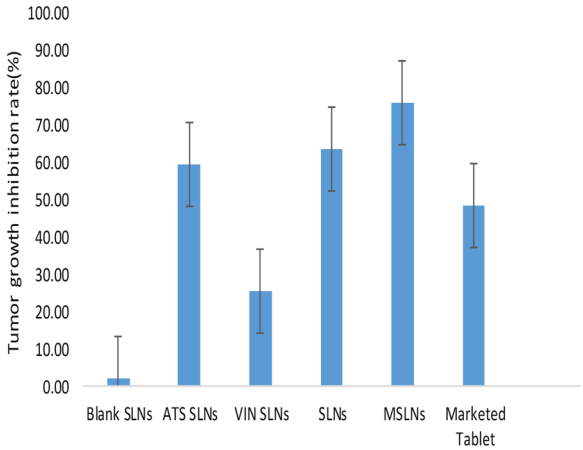

Fig. 12 Tumor inhibition rate of different formulations during treatment

0.454. The MSLNs formulation was stable till 3 months at both conditions. The results are summarized in Table 6 and student t test was used for particle size, EE for both drugs stored under refrigerated conditions and room temperature. The results gave $P \leq 0.05$ value which is insignificant for particle size, EE.

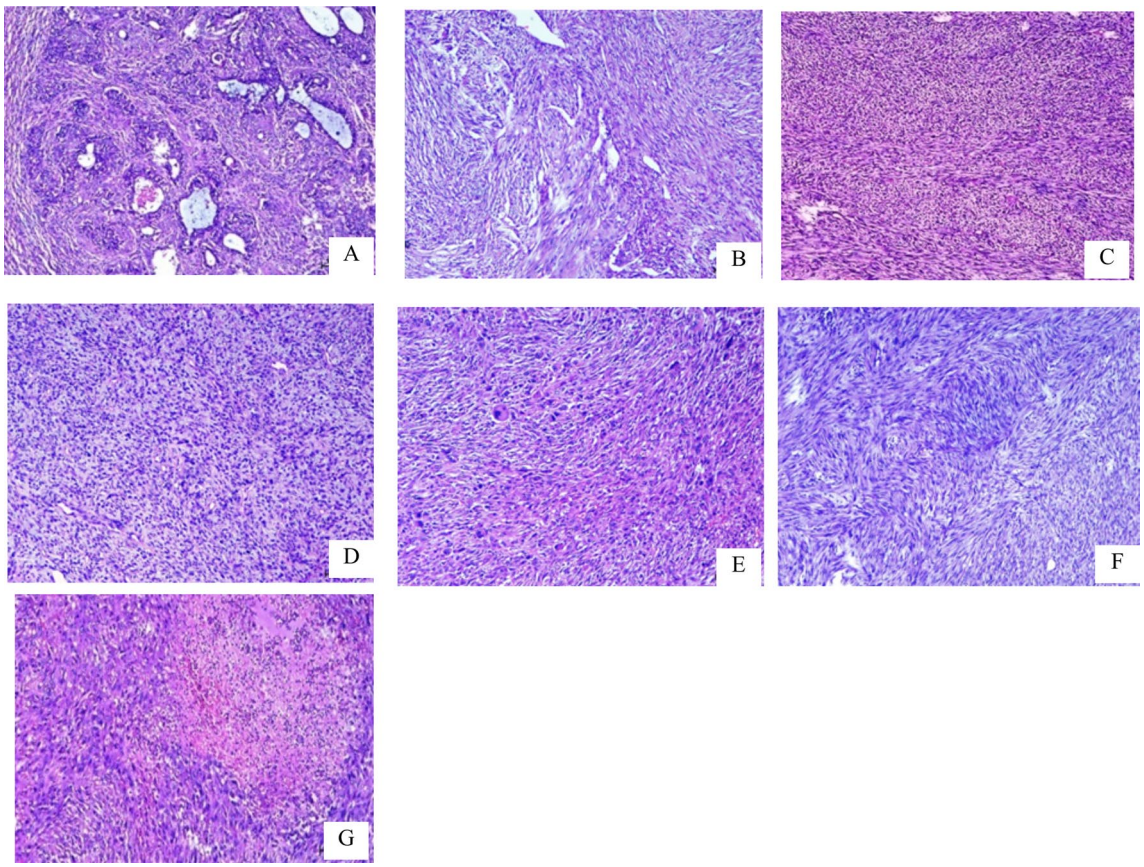

Fig. 13 Histopathology of tumor after treatment, **A** control, **B** blank SLNs, **C** ATS SLNs, **D** VIN SLNs, **E** SLNs, **F** MSLNs, **G** marketed tablet

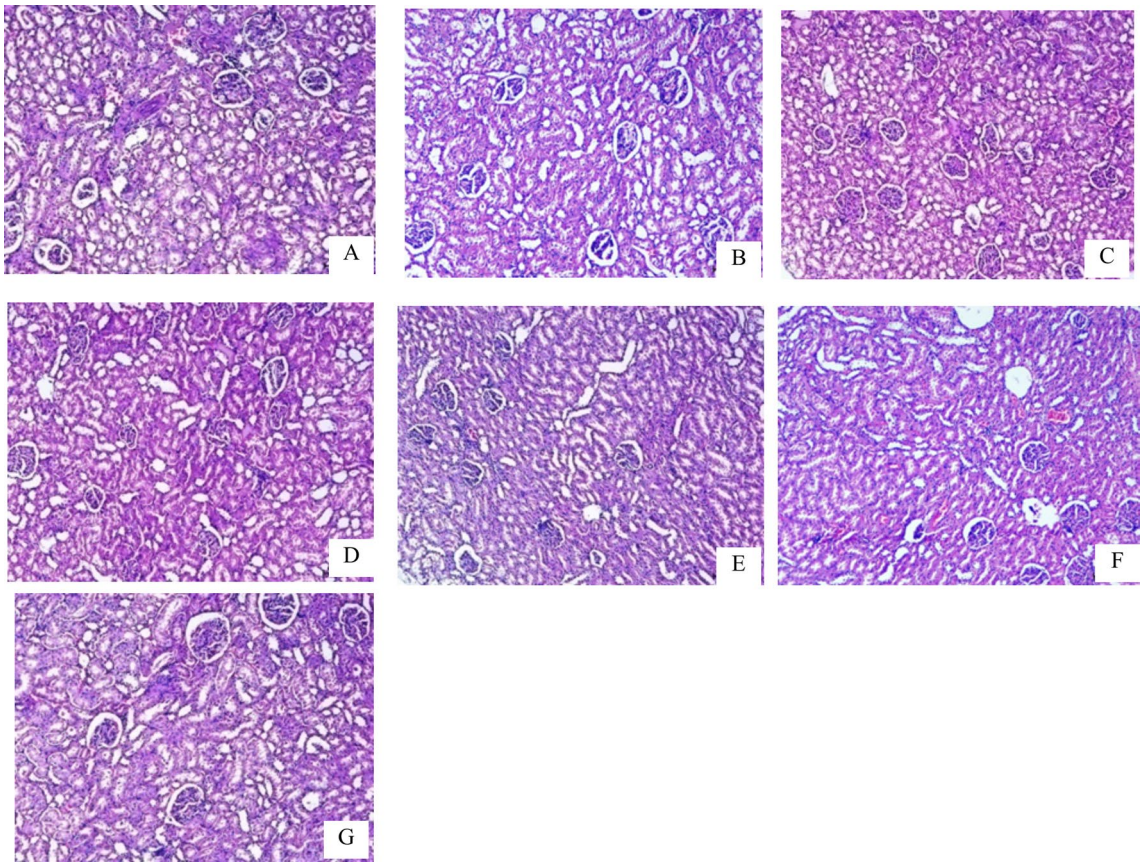

Fig. 14 Histopathology of kidney after treatment, **A** control, **B** blank SLNs, **C** ATS SLNs, **D** VIN SLNs, **E** SLNs, **F** MSLNs, **G** marketed tablet

Discussion

The PS increased after conjugation due to the surface coating of mannose on SLNs. The negative sign of ZP indicated that the formulations were stable and the value of ZP was more negative after conjugation in the MSLNs (-28.2 ± 1) due to positive charge of amine groups present on the surface of unconjugated SLNs [24]. Tween 80 and poloxamer 188 used in the formulation provided stearic stability to get the stable formulation.

The mannose-conjugation process increased the EE of MSLNs since conjugation may reduce all the deformities on the surface of SLNs [25, 26]. Mannose conjugation did not show significant change in the EE of both drugs.

MSLNs formulation exhibited significant differences in ATS and VIN as compared to SLNs due to the shield of mannose on the surface of SLNs which could be responsible for restraining the drug release from the MSLNs exhibiting a slower and sustained manner of drug release.

Free ATS and VIN were incompetent in controlling the growth rate individually and required high concentrations to show their effectiveness and due to the particle size, may unable to pass through the cell membrane. However, when both drugs were incorporated and properly encapsulated into SLNs drug delivery, required concentrations for the tumor activity was reduced. In a similar manner, SLNs and MSLN also significantly reduced the concentration to control the growth rate of MDA MB 231. SLNs enhance cellular uptake and facilitate drug release internally in a sustainable manner [27–29]. A549 cancer cells showed membrane damage and cell shrinking with condensed chromatin due to the treatment of methyl gallate and MG@Folate ZIF-L (Zeolitic imidazole framework) [30].

From the study, it is depicted that MSLNs are a suitable, efficient nano-drug delivery and appropriate for both drugs which may enhance their effectiveness by achieving target of cancer cells by augmenting permeability and passage through the cell membrane. MSLNs also showed sustained effect and hence may control the growth efficiently by receptor mediated endocytosis. ATS and VIN depicted dose dependent effect on MDA MB231 and inhibit the growth of cell lines [15, 31].

In the same way, 5 Fluouracil formulation coated with methacrylate derivatives achieve targeting in colorectal cancer. This targeted delivery tactic can boost therapeutic

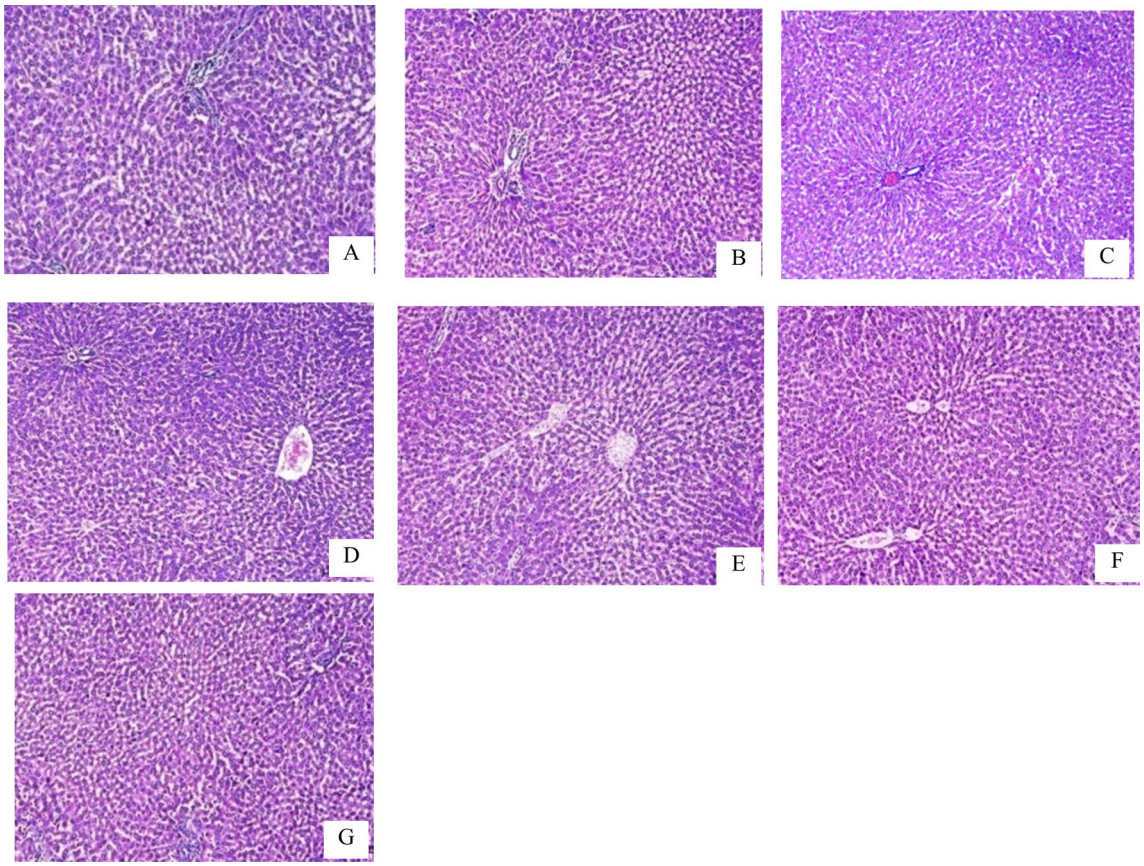

Fig. 15 Histopathology of liver after treatment, **A** control, **B** blank SLNs, **C** ATS SLNs, **D** VIN SLNs, **E** SLNs, **F** MSLNs, **G** marketed tablet

Table 6 Stability studies data

Months	Refrigerated condition*				Room temperature*			
	PS (nm)	PDI	EE (%) ATS	EE (%) VIN	PS (nm)	PDI	EE (%) ATS	EE (%) VIN
0	435.4 ± 3	0.298 ± 0.03	69.17 ± 0.92	71.18 ± 0.68	435.4 ± 3	0.298 ± 0.03	69.17 ± 0.92	71.18 ± 0.68
1	446.8 ± 5.2	0.302 ± 0.05	69.11 ± 1.30	70.56 ± 2.43	462.1 ± 6.4	0.315 ± 0.08	69.01 ± 1.41	70.46 ± 0.98
2	465.2 ± 2.61	0.334 ± 0.09	68.73 ± 2.12	70.36 ± 0.91	521.6 ± 3.2	0.398 ± 0.05	67.51 ± 0.92	70.25 ± 1.11
3	513.4 ± 6.22	0.390 ± 0.08	67.38 ± 1.74	69.72 ± 1.32	590.5 ± 2.9	0.454 ± 1.12	66.06 ± 1.26	69.12 ± 1.54

RT *$P < 0.05$ value is insignificant

efficacy of the drug and reduce dosing frequency as well as unsolicited side effects [32].

The results of in vitro cell line outcomes demonstrated that dose of individual free drug is inadequate to inhibit the 50% growth of cancer cell line. Free drugs encapsulated into the SLNs also reduced the dose of individual drugs but when both drugs were incorporated into SLNs and conjugated with mannose, it exhibited superior results by reaching the cancer cells, passing through the cell membrane and showing its effect. Due to this reason, MSLNs are effective at small doses and compared to SLNs. ATS and VIN exhibited synergism when used together and support the results of in vitro cell lines study.

All the drugs and drug-loaded SLNs, MSLNs inhibited cell growth via necrosis as well as apoptotic pathway by inducing apoptosis. VIN induces cellular apoptosis by activating mitochondria dependent pathway and disrupts the migration of MDA MB231 cells. It significantly reduces the activation of AKT and STAT3 signal transduction pathway. These mechanisms help to

suppress breast cancer. VIN also arrests the G0/G1 cell cycle phase [15]. ATS inhibits the proliferation, migration of MDA MB231 cells during induction of apoptosis [31, 33]. ATS regulates the apoptosis through PI3K/AKT signaling pathway [34]. Thus, SLNs and MSLNs showed synergistic effect by promoting to apoptosis via arresting of the Sub G1 phase. Also, they regulate AKT and STAT3 signal transduction, PI3K pathways.

Drugs are encapsulated in the lipid core such as SLNs helps to avoid the first pass effect and absorption directly through lymphatic pathway leads to increase in the bioavailability. The residence time and bioavailability was found to increase due to the incorporation of ATS and VIN in the lipid matrix when it is appropriately encapsulated in SLNs and conjugated with mannose. The slight difference between the SLNs and MSLNs formulation in the pharmacokinetic study was due to conjugation. The surface coating of mannose was available on the MSLNs which showed sustained effect up to at least 24 h. These results clearly confirmed that MSLNs would be a successful strategy to reduce the dose, frequency of drug administration and enhance therapeutic efficacy of ATS and VIN. These results of pharmacokinetic studies concluded that polysaccharide or mannose conjugated drug delivery had the potential to enhance the bioavailability in the systemic circulation. This approach helps to augment the targeting of SLNs in tumor mass. In this study it was observed that after administration of ATS and VIN together, no interaction occurs and they are simultaneously absorbed in to the systemic circulation without any interference.

Significant reduction of tumor volume was observed during treatment with MSLNs due to availability of mannose at the site of tumor cells which directly increases the intracellular uptake as well as intracellular retention of drug. The tumor regression study suggests that the combinatorial therapy showed synergistic effect more efficiently than a mono drug therapy. MSLNs boosted the tumor efficacy reaching the targeting site in minimal dose with increased survival rate, without affecting to the normal cells. In forthcoming, it may be an alternative therapy for treatment of breast cancer. It reduces the burden of side effects and makes the therapy affordable.

Conclusion

This research suggests an alternative approach to treat breast cancer by developing a combinatorial MSLNs drug delivery. In vitro release showed sustained behavior of the formulation and it was stable till 3 months. In vitro cell line results revealed that MSLNs were efficient against MDA MB231 cell line compared to the free drugs. MSLNs inhibited cell growth via necrosis as well as apoptotic pathway by inducing apoptosis and may also regulate AKT and STAT3 signal transduction pathways. MSLNs also improved the bioavailability of ATS and VIN by remaining in the blood circulation till 24 h and achieving the required therapeutic concentrations, which will be beneficial in reaching the tumor site. 76.03% tumor reduction was found for MSLNs as compared to the individual drugs and SLNs with maximal survival rate. The results concluded that MSLNs enhanced the therapeutic efficacy, reduced the dose due to combinational therapy and targeted drug delivery with minimal side effects without affecting the normal cells.

Abbreviations

ATS	Atorvastatin calcium
VIN	Vinpocetine
SLNs	Solid lipid nanoparticles
CPP	Critical process parameters
CQA	Critical quality attributes
% EE	Percent entrapment efficiency
% DL	Percent drug loading
TEM	Transmission electron microscopy
X-RD	X-ray diffraction
PDI	Poly dispersity index
ZP	Zeta potential
PBS	Phosphate-buffered saline
PS	Particle size
GMS	Glycerol monostearte
DRI	Dose reduction index
CI	Combination index
Mg	Milligram
Gm	Gram
AUC	Area under curve
MSLNs	Conjugated solid lipid nanoparticles
FT-IR	Fourier transform infra-red

Acknowledgements

We are thankful to University of Mumbai for the Minor Research Project (MRP 457/2019-20). We are grateful to DST FIST File No. SR/FST/ College 264 for FTIR and Suresh Kare Indoco Foundation for awarding the fellowship for the research work. We are thankful to ACTREC, Tata Memorial Center Navi Mumbai for providing the facility for Cancer Cell line Study and RGCB Center, Thiruvananthapuram Kerala for providing the facility for FAC study. We thank APT Center, Pune for providing the facility for in vivo tumor regression study.

Author contributions

Conceptualization, investigation, and writing RRL and ASS; methodology, validation, and data analysis RRL and ASS, experimental performance ASS. All authors have critically reviewed and approved the final submission of the manuscript. All authors read and approved the final manuscript.

Funding

Mumbai University Minor Research Project (MRP 457/2019-20) Grant received.

Availability of data and materials

The data generated or analyzed during this study are included in this article, if any excess data is required, it will be available from corresponding author on reasonable request.

Declarations

Ethics approval and consent to participate

Animal studies were conducted in accordance with procedures approved by Institutional Animal Ethics Committee with reference number KMKCP/IAEC/192007 and reference number RP 23/2021.

Consent for publication
Not applicable.

Competing interests
The authors declare no competing interests.

Received: 17 February 2023 Accepted: 23 August 2023
Published online: 21 September 2023

References

1. World Health Organization Cancer Report, USA (2021) https://www.who.int/news-room/fact-sheets/detail/cancer
2. Su CW, Chiang CS, Li WM, Hu SH, Chen SY (2014) Multifunctional nanocarriers for simultaneous encapsulation of hydrophobic and hydrophilic drugs in cancer treatment. Nanomedicine 9:1499–1515. https://doi.org/10.2217/nnm.14.97
3. Bisht S, Maitra A (2000) Dextran-doxorubicin/chitosan nanoparticles for solid tumor therapy. Adv Rev 91:415–425. https://doi.org/10.1002/wnan.43
4. Wong HL, Bendayan R, Rauth AM, Li Y, Wu XY (2007) Chemotherapy with anticancer drugs encapsulated in solid lipid nanoparticles. Adv Drug Deliv Rev 59:491–504. https://doi.org/10.1016/j.addr.2007.04
5. Jain A, Agarwal A, Majumder S, Lariya N, Khaya A, Agrawal H, Majumdar S, Agrawal GP (2010) Mannosylated solid lipid nanoparticles as vectors for site-specific delivery of an anti-cancer drug. J Control Release 148(3):359–367. https://doi.org/10.1016/j.jconrel.2010.09.003
6. Jain A, Kesharwani P, Garg NK, Jain A, Jain SA, Jain AK, Nirbhavane P, Ghanghoria R, Tyagi RK, Katare OP (2015) Galactose engineered solid lipid nanoparticles for targeted delivery of doxorubicin. Colloids Surf B Biointerfaces 134:47–58. https://doi.org/10.1016/j.colsurfb.2015.06.027
7. Ali H, Shirode AB, Sylvester PW, Nazzal S (2010) Preparation, characterization, and anticancer effects of simvastatin-tocotrienol lipid nanoparticles. Int J Pharm 389(1–2):223–231. https://doi.org/10.1016/j.ijpharm.2010.01.018
8. Osmak M (2012) Statins and cancer: current and future prospects. Cancer Lett 324(1):1–12. https://doi.org/10.1016/j.canlet.2012.04.011
9. Liu Q, Shi X, Zhou X, Wang D, Wang L, Li C (2014) Effect of autophagy inhibition on cell viability and cell cycle progression in MDAMB231 human breast cancer cells. Mol Med Rep 10(2):625–630. https://doi.org/10.3892/mmr.2014.2296
10. Anwar M, Warsi MH, Mallick N, Akhter S, Gahoi S, Jain GK, Talegaonkar S, Ahmad FJ, Khar RK (2011) Enhanced bioavailability of nano-sized chitosan-atorvastatin conjugate after oral administration to rats. Eur J Pharm Sci 44:241–249. https://doi.org/10.1016/j.ejps.2011.08.001
11. Shono N, Kin T, Nomura S, Miyawaki S, Saito T, Imai H, Nakatomi H, Oyama H, Saito N (2018) Microsurgery simulator of cerebral aneurysm clipping with interactive cerebral deformation featuring a virtual arachnoid. Oper Neurosurg 14(5):579–589. https://doi.org/10.1093/ons/opx155
12. Toepfer N, Childress C, Parikh A, Rukstalis D, Yang W (2011) Atorvastatin induces autophagy in prostate cancer PC3 cells through activation of LC3 transcription. Cancer Biol Ther 12(8):691–699. https://doi.org/10.4161/cbt.12.8.15978
13. Zhuang CY, Li N, Wang M, Zhang XN, Pan WS, Peng JJ, Pan YS, Tang X (2010) Preparation and characterization of vinpocetine loaded nanostructured lipid carriers (NLC) for improved oral bioavailability. Int J Pharm 394(1–2):179–585
14. Zhang Y, Li J (2018) An update on vinpocetine: new discoveries and clinical implications. Eur J Pharmacol 819:30–34
15. Huang EW, Xue SJ, Zhang Z, Zhou JG, Guan YY, Tang YB (2012) Vinpocetine inhibits breast cancer cells growth in vitro and in vivo. Apoptosis 17(10):1120–1130. https://doi.org/10.1007/s10495-012-0743-0
16. Lala RR, Shinde AS (2021) Development, optimization, and in vitro evaluation of atorvastatin calcium and vinpocetine codelivery by solid lipid nanoparticles for cancer therapy. Future J Pharm Sci 7:202–216. https://doi.org/10.1186/s43094-021-00351-y
17. Kumar PV, Asthana A, Dutta T, Jain NK (2006) Intracellular macrophage uptake of rifampicin loaded mannosylated dendrimers. J Drug Target 14:546–556. https://doi.org/10.1080/10611860600825159
18. Vichai V, Kirtikara K (2006) Sulforhodamine B colorimetric assay for cytotoxicity screening. Nat Protoc 1:1112–1116. https://doi.org/10.1038/nprot.2006.179
19. Skehan P, Storeng R, Scudiero D, Monks A, McMahon J, Vistica D, Warren JT, Bokesch H, Kenney S, Boyd MR (1990) New colorimetric cytotoxicity assay for anticancer-drug screening. J Natl Cancer Inst. 82:1107–1112. https://doi.org/10.1093/jnci/82.13.1107
20. Li S, Wang L, Li N, Liu Y, Su H (2017) Combination lung cancer chemotherapy: design of a PH-sensitive transferrin-PEG-Hz-lipid conjugate for the co-delivery of docetaxel and baicalin. Biomed Pharmacother 95(27):548–555. https://doi.org/10.1016/j.biopha.2017.08.090
21. Elmowafy M, Ibrahim HM, Ahmed MA, Shalaby K, Salama A, Hefesha H (2017) Atorvastatin-loaded nanostructured lipid carriers (NLCS): strategy to overcome oral delivery drawbacks. Drug Deliv 24(1):932–941. https://doi.org/10.1080/10717544.2017.1337823
22. Sahu PK, Mishra DK, Jain N, Rajoriya V, Jain AK (2015) Mannosylated solid lipid nanoparticles for lung-targeted delivery of paclitaxel. Drug Dev Ind Pharm 41(4):640–649. https://doi.org/10.3109/03639045.2014.891130
23. Horter D, Dressman JB (2001) Influence of physicochemical properties on dissolution of drugs in the gastrointestinal tract. Adv Drug Deliv Rev 46:75–87. https://doi.org/10.1016/S0169-409X(00)00130-7
24. Vieira ACC, Chaves LL, Pinheiro M, Ferreira D, Sarmento B, Reis S (2016) Design and statistical modeling of mannose-decorated dapsone-containing nanoparticles as a strategy of targeting intestinal m-cells. Int J Nanomed 11:2601–2617. https://doi.org/10.2147/IJN.S104908
25. Vieira ACC, Chaves LL, Pinheiro M, Lima SAC, Ferreira D, Sarmento B, Reis S (2018) Mannosylated solid lipid nanoparticles for the selective delivery of rifampicin to macrophages. Artif Cells Nanomed Biotechnol 46:653–663. https://doi.org/10.1080/21691401.2018.1434186
26. Pinheiro M, Ribeiro R, Vieira A, Andrade F (2016) Design of a nanostructured lipid carrier intended to improve the treatment of tuberculosis. Drug Des Devel Ther. 10:2467–2475. https://doi.org/10.2147/DDDT.S104395
27. Subedi RK, Kang KW, Choi HK (2009) Preparation and characterization of solid lipid nanoparticles loaded with doxorubicin. Eur J Pharm Sci 37:508–513. https://doi.org/10.1016/j.ejps.2009.04.008
28. Fundaro A, Cavalli R, Bargoni A, Vighetto D, Zara GP, Gasco MR (2000) Non-stealth and stealth solid lipid nanoparticles (SLN) carrying doxorubicin: pharmacokinetics and tissue distribution after i.v. administration to rats. Pharmacol Res. 42:337–343. https://doi.org/10.1006/phrs.2000.0695
29. Serpe L, Catalano MG, Cavalli R, Ugazio E, Bosco O, Canaparo R, Muntoni E, Gasco MR, Eani M, Zara GP, Frairia R (2004) Cytotoxicity of anticancer drugs incorporated in solid lipid nanoparticles on HT-29 colorectal cancer cell line. Eur J Pharm Biopharm 58:673–680. https://doi.org/10.1016/j.ejpb.2004.03.026
30. Marji SM, Bayan MF, Jaradat A (2022) Facile fabrication of methyl gallate encapsulated folate ZIF-L nanoframeworks as a pH responsive drug delivery system for anti-biofilm and anticancer therapy. Biomimetics 7:242. https://doi.org/10.3390/biomimetics7040242
31. Hu MB, Zhang JW, Gao JB, Qi YW, Gao Y, Xu L, Ma Y, Wei ZZ (2018) Atorvastatin induces autophagy in MDA MB231 breast cancer cells. Ultrastruct Pathol 42(5):409–415. https://doi.org/10.1080/01913123.2018.1522406
32. Bayan MF, Jaradat A, Alyami MH, Naser AY (2023) Smart pellets for controlled delivery of 5-fluorouracil. Molecules 28(1):306. https://doi.org/10.3390/molecules28010306
33. Ma Q, Gao Y, Xu P, Li K, Xu X, Gao J, Qi Y, Xu J, Yang Y, Song W (2019) Atorvastatin inhibits breast cancer cells by downregulating PTEN/AKT pathway via promoting Ras homolog family member B (RhoB). Biomed Res Int 2019:3235021. https://doi.org/10.1155/2019/3235021
34. Docrat TF, Nagiah S, Krishnan A, Naidoo DB, Chuturgoon AA (2018) Atorvastatin induces MicroRNA-145 expression in HEPG2 Cells via regulation of the PI3K/AKT signalling pathway. Chem Biol Interact 287:32–40. https://doi.org/10.1016/j.cbi.2018.04.005

Publisher's Note